AN INSIGHT OF THE SUBSURFACE THROUGH BOREHOLE IMAGES CASE STUDY OF MW-34 MENENGAI GEOTHERMAL FIELD, KENYA.

Marietta Mutonga [1] and Fujimitsu Yasuhiro[1],

Geothermal Development Company (GDC), P.O Box 100746, 00101, Nairobi Kenya

Kyushu University, ITO Campus, 744 Motooka, Nishi Ward, Fukuoka, 819-0395, Japan.

mariettamu@gmail.com/ mutonga.marietta.200@s.kyushu-u.ac.jp

fujimitsu@mine.kyushu-u.ac.jp

Keywords: *Borehole images, Fractures, Subsurface, Menengai.*

ABSTRACT

Borehole imaging has been one of the fast-evolving technologies in well logging. The understanding of geological formations and logged formations below the surface has greatly improved since the advent of borehole imaging tools. The presence of natural fractures provides important pore spaces and fluid flow conduits. Insights can be provided into the subsurface fracture (natural and induced) detection and characterization using image logs. Menengai Geothermal field is quaternary volcano located in the central part of the Kenya rift which hosts a high temperature geothermal system. No core has been acquired from any of the wells drilled in this field. Therefore, to have a better understanding of the subsurface, a few wells were selected for borehole imaging. There are different methods of acquiring borehole images that include; Optical , acoustic and micro-resistivity. In this study, acoustic borehole-imaging devices were used to image MW-34, a vertical well drilled in NE part of the Menengai Geothermal field in Kenya. with the QL 43 ABI device. This device is also known as "borehole televiewers." It operates with pulsed acoustic energy so that it can image the borehole wall within drilling fluids. Using WellCad Software to analyze the borehole image we were able to recognize structures through irregularities on the borehole wall. The structures were captured from the image by fitting sinusoids to discontinuity traces. Numerous low acoustic amplitude fractures, which appeared as dark sinusoids, were noted in the depths ranging from 1370-1380 m and from 1530-1550 m. A few large apparent apertures fractures have been noted with the largest of 1160.69 mm in size, some lithological contacts have also been noted and appear to be low acoustic amplitude at 1180 m and 2275 m among other depths. Generally, the fracctures have a strike orientation of NE-SW.

1. INTRODUCTION

Menengai geothermal field is located, in the central part of the Kenyan Rift approximately 10 km from Nakuru Town and about 20 km to Lake Nakuru. It's host to a high temperature geothermal system. More than 40 wells have been drilled in this field leading to a better understanding of the geothermal reservoir. Mapping is the essence of geology. Geology maps provide the wherewithal to decrypt the time and space organization of Earth's solid and fluid spheres. We map the exterior surface by directly observing rocks and fluids, 'walking out' rock units, measuring, sampling and imaging as we go. The formations mapped within the caldera and those intersected by the wells are of peralkaline trachytic composition, presumably derived from fractionation of basaltic magmas, and consist predominantly of lavas, with subordinate pyroclastic intercalations and with a progressive increase of intrusive products towards the wells bottom as has been revealed by wells drilled (Mibei, 2015). Subsurface mapping is the essence of all explorations for aquifers, hydrocarbons, minerals, geothermal energy and geotechnical constructions, it provides us with an understanding of how the Earth works. The understanding of geological formations and logged formations below the surface has greatly improved since the advent of borehole imaging tools (Folkestad et al., 2012). A detailed account of location, orientation and nature of fractures is afforded by acoustic borehole imager. In normal practice, cores are taken during the exploration stage. However, in many parts of the world this is not always practical Menengai geothermal field is not an exception, No core had been previously studied in this field due to time and capital constraints, therefore, to better understand the subsurface, a few wells were identified for borehole imaging. In this paper we introduce MW-34, a vertical well that has been drilled to 2916 m CT. The well was drilled to with the aim of further extending North Eastern part of the geothermal field (Figure 1). The 8 1/2" production section was imaged from1148-2399 m CT (Cellar Top). The well could not be imaged beyond this point because of the prevailing well conditions (i.e., the well was too hot for the tool). The QL 43 ABI device used works in temperatures 0-125ºC and pressures up to 700 bars. The formations encountered include trachyte, trachyte & tuff intercalations, and the intrusive formation equivalent of trachyte syenite. Fractures have been identified throughout the imaged section of the well with an average dip orientation of NE- SW (Figure 2).

ISSN 2703-4275

Figure 1: Location of MW-34 within the Menengai Caldera; white outline (right), inset its location in relation to the Kenyan Rift (`N-S) and the Nyanzian Rift(E-W) (left)

1.1 Geological Setting

Menengai Geothermal field is located the in the Menengai Caldera which is located central part of the Kenyan rift. This is a zone of abnormal mantle material which coincides with an area of crustal upwarping commonly referred to as the Kenya Dome (Smith,1994). The Kenya Dome (Figure 1) was the focus of much of the Neogene magmatism in the southcentral part of the rift (Macdonald, 2002). The caldera is located right at the triple junction where the more developed Kenyan Rift intersects with the ENE-WSW Nyanzian rift, which at that same point, changes its direction from NNE-SSW to NW-SE (Chorowicz, 2005). Menengai Caldera is one of the Quaternary volcanoes formed on the axis of the Kenyan rift. It is a trachytic central volcano that is underlain by a high-level magma chamber (Leat and Macdonald, 1984). The formation of the Caldera started around 200 Ka with the building up of a 30 km^3 lava shield volcano with a NNW-SSE orientation(Leat, 1983). The formation of the caldera was proceeded by the two major volcanic eruptions, the first in 29 Ka and the second one in 8 Ka which resulted in a caldera 12 km by 8 km being formed (Figure 2). There is a well-developed sector graben, embayed caldera walls, and apparently random spacing of some post-caldera vents indicating piecemeal (Krakatoan) collapse (Leat and Macdonald, 1984). More than 70 post caldera lava flows erupted cover the caldera floor (Figure 1(right), in volume they represent 23 km^3 of magma.

2.0 METHODS

2.1 Image Logging

Borehole imaging tools afford an image of the borehole wall that is naturally based on physical property disparities. There are different methods of acquiring borehole images that include: optical , acoustic and micro-resistivity imaging. In this study acoustic borehole-imaging devices have been used to image MW-34 a vertical well drilled in NE part of the Menengai geothermal field in Kenya with the QL 43 ABI device. Acoustic image logs provide an oriented image of the inside of the borehole, with an image resolution of the order of $\leq$ 1m (Massiot et al., 2015). Acoustic imaging tools exploit a piezoelectric transducer that produces a focused high frequency sonic pulse to the borehole wall (Asquith and Krygowski, 2004; Tingay et al., 2008). Short bursts of acoustic energy are emitted by a rotating transducer in pulse-echo mode. These travel through the drilling fluids and undergo partial reflection at the borehole wall. Reflected pulses are received by the transducer. The acoustic imaging tool records amplitude of the return echo as well as the total travel time of the sonic. The amplitudes of the reflected pulses form the basis of the acoustic image of the borehole wall. The amplitudes are governed by several factors. The first is the shape of the borehole wall itself: irregularities cause the reflected energy to scatter so that a weaker reflected signal is received by the transducer. Second is properties of minerals and borehole wall formation.

The sonic travel-time and amplitude signals provide information on borehole shape and variation in rock properties. They are visualized as unrolled 360° images of the borehole wall (Massiot et.al., 2015). The acoustic wave travel time and reflected amplitudes are measured at numerous azimuths inside the wellbore for any given depth. This data is then processed into images of the borehole wall reflectance (based on return echo amplitude) and borehole radius (based on pulse travel time; Tingay et.al., 2008).

1.2.1 Image log processing

Before analysis is performed, the data needs to be processed. This involves the creation of a reliable high-quality image from raw tool measurements. Several processing options are available for enhancing the quality of the data (Well Cad software processing manual)

These include:

- Bad trace interpolation
- Image normalization
- Centralize image
- Adjust brightness and contrast (for RGB logs)

Static normalization images are used to correlate lithological changes over an entire well, while dynamic normalization is used for detailed assessments of fractures (Wilson et al., 2013). For both travel time and amplitude, static and dynamic normalizations were applied to for travel time and amplitude images (Figure 4 & 5). However, minor differences were noted on the displays therefore both statically and dynamically normalized borehole images were used to identify the structural features, such as fractures. Planar features were manually picked by fitting sinusoid in WellCad.

The acoustic image enabled us to identify natural fractures. We used criteria according to Niu et al., 2019 (cement-filled (closed) fractures are commonly detected by image logs as bright discontinuous sinusoidal waves due to resistive filling materials, while the open fractures are evident on image logs appearing as dark sine wave) to pick fractures. Image analysis was performed manually, without using any automatic picking algorithms, thus increasing the quality of the analysis; fractures were picked from dynamically normalized image logs by manually tracing sine waves. Picked fractures are presented as tadpoles in Figure 3,4 & 6.

2. RESULTS

The fractures interpreted from image logs can be classified in two types: natural and induced fractures. In this Paper we based only on natural fractures. Natural fractures are defined as the fractures in a formation prior to drilling (Nelson, 2001). Induced features were formed through drilling and the existence of the borehole itself (Zoback et.al., 2003; Massiot et.al., 2015).

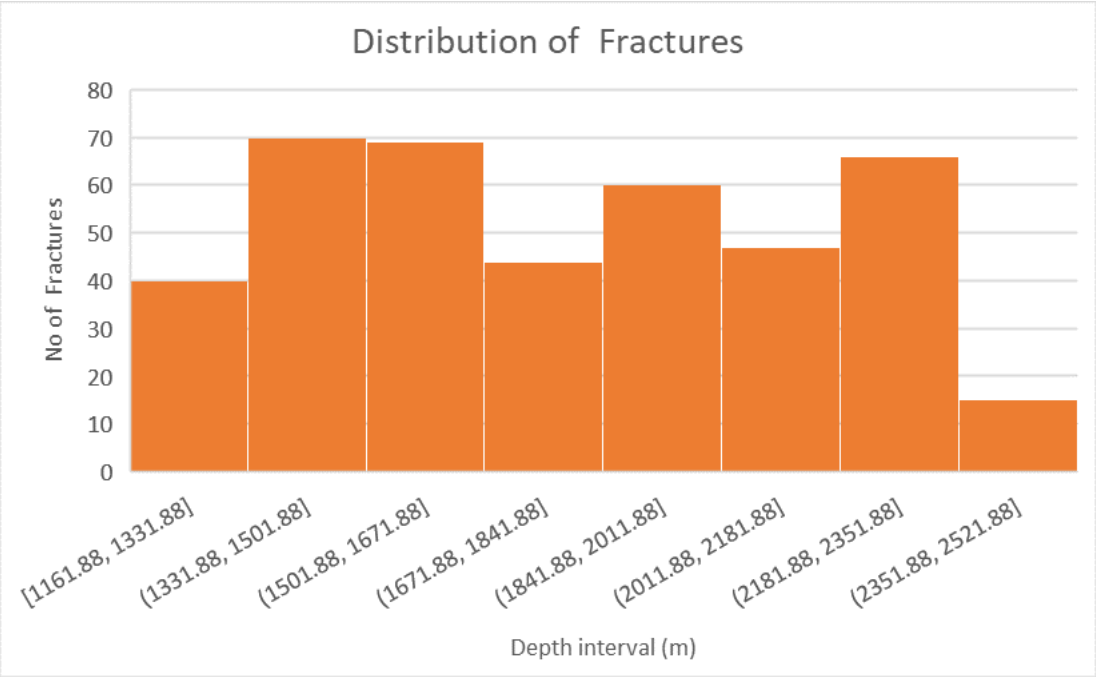

Figure 2: Distribution of fractures every 170 m

ISSN 2703-4275

Fractures are well developed over almost the entire logged interval with 40 fractures picked per every 170 m long interval (Figure 2) with varying orientations. The fractures have NE-SW strike orientation with high dip angles that are mostly dips above 75º with dip directions mostly greater than 300º. The fractures are more abundant within the trachyte-tuff intercalations formations e.g. At 2340 m (Figure 4), while there's scarcity of fractures within the syenite formation an intrusive formation. Syenite appears as fresh and coarse grained when it's not altered or fractured, mainly at the deeper parts of this well from 2280-2335 m (Figure 3).

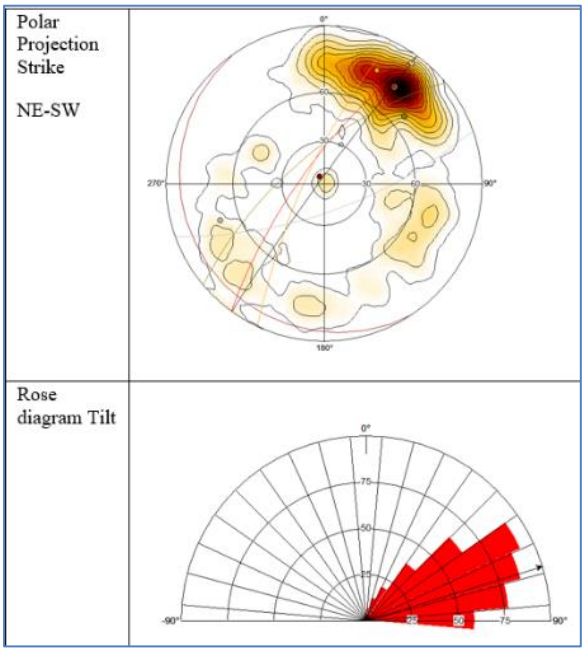

Figure 3 : Mean Dip and Strike of MW-3

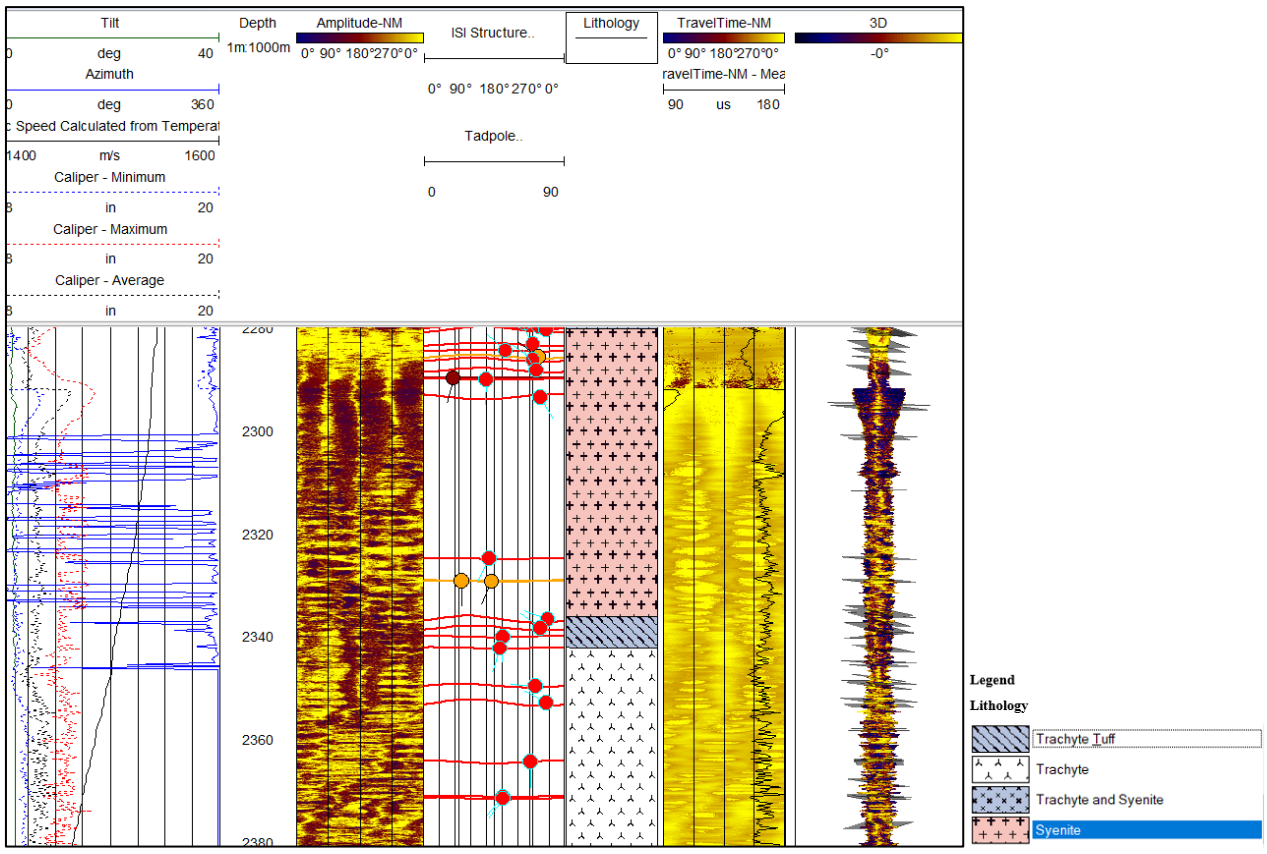

Figure 4: Formation encountered in MW-34

ISSN 2703-4275

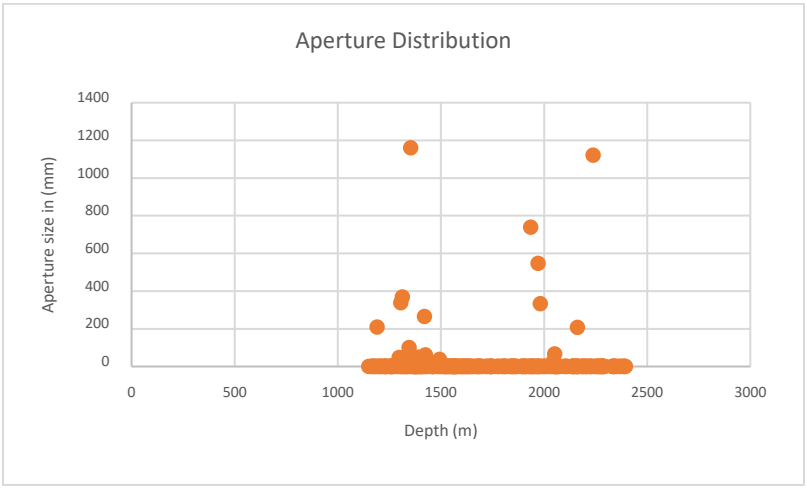

Figure 5: Aperture distribution within MW-34

Between fracture parameters, the aperture has the greatest effect on reservoir properties especially permeability (Aghli et. al., 2014 in Lai 2018). Apertures are gaps or openings or open spaces within fractures (Figure 5 and 6) that are assumed to be fluid filled because they have dark thick sinusoidal stripes in the amplitude and travel time logs which is a likely indication that they extend beyond the borehole wall. In this paper fracture openings greater than 100mm(10cm) were apertures. Fluid filled fractures also act as sources of tube waves traveling upward and downward along the borehole, starting from the given fracture location (Figure 4). When picking out apertures a conservative approach was taken because the automatic picking proved to be chaotic, unreliable, and not accurate. As a result, apertures picked were very few but representative of the actual structural condition of the well. Most apparent apertures >100mm seem to be concentrated around 1200-1500 m and 1800-2300 m (Figure 5). The apparent apertures > 100mm vary from being partially to fully seen on the travel time image. Good examples include two fractures with large apparent apertures that have sizes; 1121.697 mm (a found at a depth of 2238.37 m with a dip direction of 136.7^{o} and dip magnitude of 63.6^{o}) and 1160.69 mm (found at a depth of 1354 m with a dip direction of 12^{o} and dip magnitude of 45^{o}). The apparent apertures seem to tally with the high rates of penetration (ROPs) of the drill bit and Travel time image logs (Figure 6). Even though some fractures with increased apparent apertures may appear to have partial spalling from the borehole wall, they may be open to fluid flow.

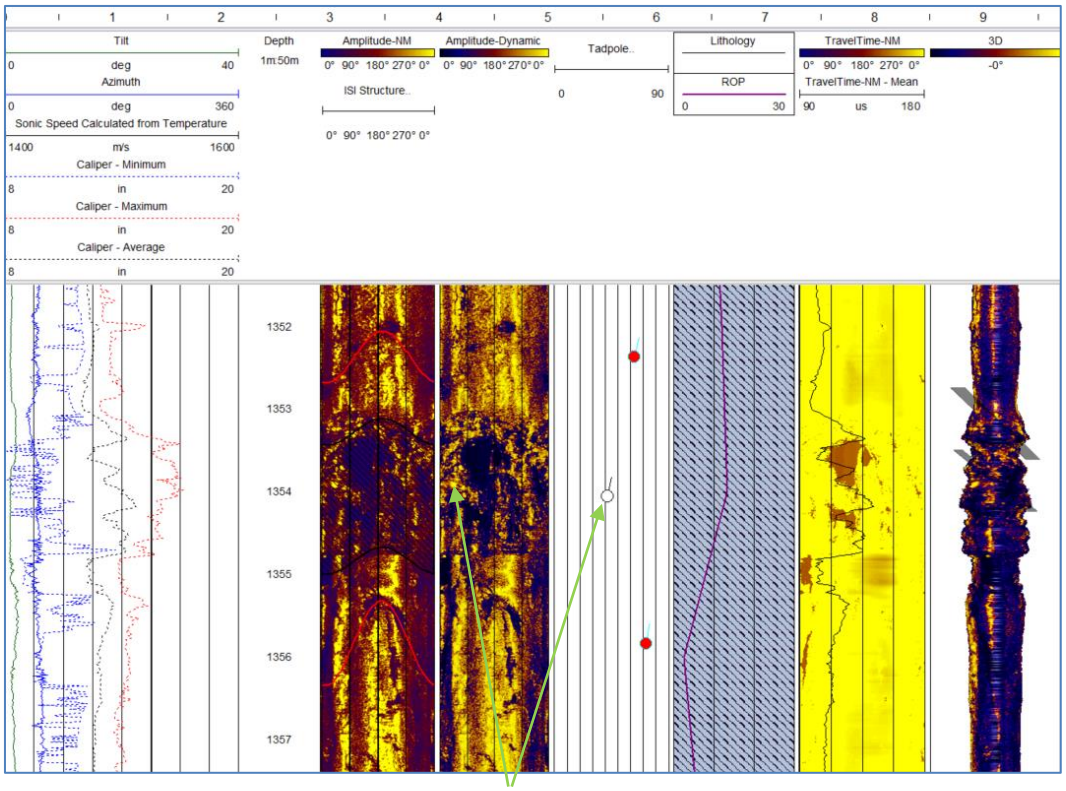

Figure 6: Open apertures

ISSN 2703-4275

3. DISCUSSIONS AND CONCLUSION

In this study acoustic borehole-imaging devices have been used to image MW-34 a vertical well drilled in NE part of the Menengai Geothermal field in Kenya with the QL 43 ABI device which works in temperatures 0-125 ºC and pressures up to 700 bars. From the borehole image we note that fractures are well developed over almost the entire logged interval of this well i.e., from 1195 - 2400 m CT. In this paper we based our study on natural fractures. Low acoustic amplitude fractures, especially those seen on the travel time, have the potential to allow fluid to flow through them while high amplitude acoustic amplitude fractures do not allow fluid to flow. The widest apparent apertures were picked manually. These fractures have higher potential to have open spaces or voids between two fractures. Most high apparent aperture fractures seem to be concentrated around 1200-1500m and 1800-2300 m. The apparent apertures are >1m, this could be fractured zones that relate to faults observed at the surface in Menengai geothermal field.

4. ACKNOWLEDGEMENTS

We wish to thank GDC (Geothermal Development Company) for data access and my study leave, JICA (Japan International Corporation) for the Scholarship, West-Jec (West Japan Engineering Consultants, Inc) for organizing the training on the WellCAD Software and Alt (Advanced Logic Technology) for sponsoring the WellCAD software.

5. REFERENCES

Asquith, G. & Krygowski D., 2004: Basic well log analysis. - AAPG Methods in Exploration 16, AAPG, Tulsa, Oklahoma, 244 p.

Chorowicz, J., 2005: The mechanisms of the East African Rift System formation. J. African Earth Science, 43, pp. 379-410.

Niu H., Liu,S., Lai,J., Wang, G., Liu,B., Xie, Y., and Xie, W., 2019: In-situ stress determination and fracture characterization using image logs: The Paleogene Dongying Formation in Nanpu Sag, Bohai Bay Basin, China

Folkestad, A., Veselovsky, Z., & Roberts, P., 2012: borehole image logs to interpret delta to estuarine system: a case study of the subsurface Lower Jurassic Cook Formation in the Norwegian northern North Sea Mar. Petrol. Geol., 29, pp. 255-275.

Kahiga,E., 2014 Significance of Tectono-volcani Axes in Menegai Geothermal. Field Proceedings 5th African Rift Geothermal Conference (ARGEO) Arusha, Tanzania, 29-31st October 2014.

Lai, J., Wang ,G., Wang, S., Cao, J., Li, M., Pang, X., Han, C., Fan, X., Yang ,L., He, Z. Qin Z., 2018: A review on the applications of image logs in structural analysis and sedimentary characterization. Marine and Petroleum Geology Vol.95, August 2018, pp. 139-166.

Leat, P, T., and Ray Macdonald, R., 1984: Geochemical Evolution of the Menengai Caldera Volcano, Kenya Journal of Geophysical Research, Vol. 89, no. b10, pp. 8571-8592, Sept 30, 1984.

Leat T.P., 1983 The structural and geochemical evolution of Menengai Caldera volcano, Kenya Rift *Valley. Univ. of Lancaster, Lancaster, UK, PhD thesis.*

MacDonald, R., 2002: Magmatism of the Kenya Rift Valley: a review Transactions of the Royal Society of Edinburgh: Earth Sciences, 93, pp. 239-253, 2003 (for 2002).

Massiot, C., Mcnamara, D.D., & Lewis, B., 2015: Processing and analysis of high temperature geothermal acoustic borehole image logs in the Taupo volcanic zone, New Zealand Geothermics, 53, pp. 190-201.

Mibei, G., Njue, L., and Ndongoli, C., Geothermal exploration of the Menengai geothermal field proceedings, 6th African Rift Geothermal Conference (ARGEO)Addis Ababa, Ethiopia, 2nd -4th Nov 2016

Nelson, R., 2001: Geologic Analysis of Naturally Fractured Reservoirs Gulf Professional Publishing, pp. 96-104.

Niu H., Liu S., Wang G., Liu B., Xie Y., and Xie W., 2020: In-situ stress determination and fracture characterization using image logs: The Paleogene Dongying formation Nangpu Sag, Bohai Bay Basin, China. Energy Science Engineering 2020; Vol.8 Issue 2, pp. 476-489.

Smith, M., 1994: Stratigraphic and structural constraints on mechanisms of active rifting in the Gregory Rift, Kenya. Tectonophysics 236, pp 3-22.

Tingay, M., Reineker, J., and Muller, B., 2008: Guidelines: Image Logs World Stress Map 2008.

WellCAD© Basic Version 5.4 Well Log Processing Software manual

Wilson, M, E, J., Lewis. D., Yogi, O., Holland, D., Hombo, L., & Goldberg, A., 2013: Development of a Papua New Guinean onshore carbonate reservoir: a comparative borehole image (BHI) and petrographic evaluation. Mar. Petrol. Geol., 44 , pp. 164-195.

Zoback, M., Barton, C., Brudy, M., Castillo, D., T. Finkbeiner, T., Grollimund, B., Moos, Peska, P., Ward, C., and Wiprut, D.,2003: Determination of stress orientation and magnitude in deep wells Int. J. Rock Mech. Min. Sci., 40, pp. 104

ISSN 2703-4275